EXHIBIT E

0090-9556/97/2507-0863-872$0000/0
DRUG METABOLISM AND DISPOSITION
Vol. 25, No. 7
Printed in U.S.A.

METABOLISM AND EXCRETION OF A NEW ANTIPSYCHOTIC DRUG, ZIPRASIDONE, IN HUMANS

CHANDRA PRAKASH, AMIN KAMEL, JUDITH GUMMERUS, AND KEITH WILNER

Departments of Drug Metabolism (C.P., A.K.) and Clinical Research (J.G., K.W.), Central Research Division, Pfizer, Inc.

(Received December 12, 1996; accepted April 1, 1997)

ABSTRACT:

The pharmacokinetics, metabolism, and excretion of a new antipsychotic drug, ziprasidone, were studied in four normal male volunteers after oral administration of a single 20 mg dose of a mixture of ^{14}C- and ^{3}H-labeled ziprasidone. Blood, urine, and feces were collected at various intervals for determination of total radioactivity and metabolic profiles. Eleven days after the dose, 20.3 ± 1% of the administered radioactivity was recovered in the urine and 66.3 ± 4.8% in feces. The absorption of ziprasidone was rapid, and the C_{max} for ziprasidone and metabolites occurred at 2 to 6 hr postdose. Mean peak serum concentration of unchanged drug was 45 ng/ml and a mean $AUC_{(0-t)}$ of 335.7 ng · hr/ml. Mean peak serum concentration of total radioactivity (average of ^{3}H and ^{14}C) was 91 ng-eq/ml and a mean $AUC_{(0-t)}$ of 724.6 ng-eq · hr/ml. On the basis of $AUC_{(0-t)}$ values, ~46% of circulating radioactivity was attributable to unchanged drug.

Ziprasidone was extensively metabolized and only a small amount (<5% of the administered dose) was excreted in urine and feces as unchanged drug. Twelve metabolites in human urine and serum were identified by ion-spray LC/MS and LC/MS/MS with simultaneous monitoring of radioactivity. The major urinary metabolites were identified as oxindole-acetic acid and its glucuronide conjugate, benzisothiazole-3-yl-piperazine (BITP), BITP-sulfoxide, BITP-sulfone and its lactam, ziprasidone-sulfoxide, and sulfone similar to those identified in rats. In addition, two novel metabolic pathways (reductive cleavage and *N*-dearylation of the benzisothiazole ring) were identified for ziprasidone in humans. The metabolites resulted by these pathways were characterized as *S*-methyl-dihydro-ziprasidone, *S*-methyl-dihydro-ziprasidone sulfoxide, and 6-chloro-5-(2-piperazin-1-yl-ethyl)-1,3-dihydro-indol-2-one, respectively. Ziprasidone sulfoxide and sulfone were the major metabolites in human serum. The affinities of the sulfoxide and sulfone metabolites for 5-HT_2 and D_2 receptors are low with respect to ziprasidone, and are thus unlikely to contribute to its antipsychotic effects. Structures of the major metabolites were confirmed by chromatographic and spectroscopic comparisons to synthetic standards. Based on the structures of these metabolites, four routes of metabolism of ziprasidone were identified: *1)* *N*-dealkylation of the ethyl side chain attached to the piperazinyl nitrogen, *2)* oxidation at sulfur resulting in the formation of sulfoxide and sulfone, *3)* reductive cleavage of the benzisothiazole moiety, and *4)* hydration of the C=N bond and subsequent sulfer oxidation or *N*-dearylation of the benzisothiazole moiety. The identified metabolites accounted for >90% of total radioactivity recovered in urine.

ZIP,[1] an effective antipsychotic, has a unique collection of receptor affinities (1–4). In conjunction with a high 5-HT_2/D_2 receptor antagonist ratio, it has potent affinity for 5-HT_{1a}, 5-HT_{1d}, and 5-HT_{2c} receptors and moderately inhibits norepinephrine and 5-HT reuptake that favors both improved toleration and expanded antipsychotic efficacy (3, 4). The compound is under late phase III clinical trials for the treatment of schizophrenia. Its preclinical and clinical pharmacological profiles suggested that ZIP should be effective in the treatment of both positive and negative symptoms of schizophrenia (3, 4). In phase III clinical studies, ZIP has demonstrated good tolerability, particularly with regard to extrapyramidal side effects, at doses that are associated with efficacy in patients with schizophrenia (5). The oral bioavailability of ZIP in human is 59%, and its elimination half-life is 4 hr (6).

The metabolism, excretion, and pharmacokinetics of ZIP in rats and dogs after a single oral dose have been reported recently (7–9). ZIP is partially absorbed in rats and dogs with absolute oral bioavailability ranging from 39 to 60%. The elimination half-life is ~1 hr in both male and female rats, and 2.3 hr in male dogs (7). ZIP is extensively metabolized in rats and dogs. The main metabolic pathways were the *N*-dealkylation of the ethyl group attached to the piperazinyl nitrogen and oxidation at sulfur of the benzisothiazole ring (8, 9). Data on the biotransformation of ZIP in humans are required to characterize human disposition and to compare with animal data. The aim of the present study was to determine the excretion routes in humans for ZIP and its metabolites, to elucidate the metabolic pattern of ZIP, and to evaluate pharmacokinetic parameters of ZIP and metabolites. A mixture of ZIP labeled with ^{14}C at C-2 of the ethyl group attached to the piperazinyl nitrogen, and ^{3}H at the C-7 position of the benzisothiazole

This work was presented in part at the 4th International Society for the Study of Xenobiotics Meeting, Seattle, WA, 1995.

[1] Abbreviations used are: ZIP, ziprasidone (5-[2-[4-(1,2-benzisothiazol-3-yl)-piperazin-1-yl]ethyl]-6-chloro-1,3-dihydro-indol-2-one) hydrochloride hydrate; 5-HT, 5-hydroxytryptamine; $TiCl_3$, titanium (III) chloride; radio-HPLC, HPLC with on-line radioactivity detection; ZIP-SO, ziprasidone sulfoxide; ZIP-SO_2, ziprasidone sulfone; OX-AA, (6-chloro-2-oxo-2,3-dihydro-1*H*-indol-5-yl)acetic acid; BITP, 3-(piperazine-1-yl)-1,2-benzisothiazole; BITP-SO, BITP sulfoxide; BITP-SO_2, BITP-sulfone; OX-P, 6-chloro-5-(2-piperazin-1-yl-ethyl)-1,3-dihydro-indol-2-one; dihydro-ZIP, 6-chloro-5-(2-{4-[imino-(2-mercapto-phenyl)methyl]-piperazin-1-yl}ethyl)-1,3-dihydro-indol-2-one; *S*-methyl-dihydro-ZIP, 6-chloro-5-(2-{4-[imino-(2-methylsulfanyl-phenyl)methyl]-piperazin-1-yl}ethyl)-1,3-dihydro-indol-2-one; *S*-methyl-dihydro-ZIP-SO, 6-chloro-5-(2-{4-[imino-(2-methyl-sulfanyl-phenyl)-methyl]-piperazin-1-yl]ethyl}-1,3-dihydro-indol-2-one-*S*-oxide; AUC, area under the serum concentration-time curves; C_{max}, maximum concentration; t_{max}, time to maximum concentration; β-RAM, radioactivity monitor; CID, collision-induced dissociation; CNL, constant neutral loss; MRM, multiple reaction monitoring; MTBSTFA, N(tert-butyldimethylsilyl)-*N*-methyltrifluoroacetamide; 5-OH-ZIP, 5-hydroxy-ziprasidone; TIC, total ion current; RAD, radioactivity detector; dihydro-ZIP-O_2, 2-{4-[2-(6-chloro-2-oxo-2,3-dihydro-1*H*-indol-5-yl)-ethyl]-piperazine-1-carbonyl}-benzenesulfinic acid amide.

Send reprint requests to: Dr. Chandra Prakash, Department of Drug Metabolism, Central Research Division, Pfizer, Inc., Groton, CT 06340.

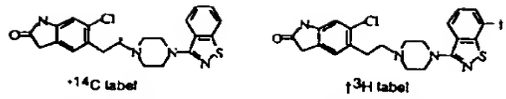

FIG. 1. *Structures of ^{14}C- and ^{3}H-labeled ZIP.*

was administered to normal healthy male volunteers (fig. 1). The use of two labels at these positions greatly facilitated the tracing and identification of metabolites that were formed through cleavage of ZIP similar to that reported for structurally related drug tiospirone (10, 11). Structure elucidation of the major metabolites was achieved by LC/MS/MS with radioactivity monitoring, and identities of several metabolites were confirmed unambiguously by comparison of their chromatographic and spectral behaviors with those of synthetic standards.

Materials and Methods

General Chemicals. Commercially obtained chemicals and solvents were of HPLC or analytical grade. β-Glucuronidase (from *Helix pomatia*, type H-1 with sulfatase activity) was obtained from Sigma Chemical Company (St. Louis, MO). YMC basic columns were obtained from YMC (Wilmington, NC). Ecolite (+)-scintillation cocktail was obtained from ICN (Irvine, CA). Carbosorb, Monophase S, and Permafluor E+ scintillation cocktails were purchased from Packard Instrument Company (Downers Grove, IL). $TICl_3$ solution (20%) was obtained from Fisher Scientific (Springfield, NJ).

Radioactive Drug and Reference Standards. A mixture of ^{3}H- and ^{14}C-labeled ZIP (specific activity: 2.11 mCi for ^{3}H and 1.12 mCi for ^{14}C per mmol) was prepared at Pfizer Central Research by the radiochemistry group as described (12). It showed a radiopurity of 99% for both labels (radio-HPLC). ZIP-SO, ZIP-SO_2, OX-AA, BITP, BITP-SO, BITP-SO_2, BITP-SO_2-lactam, and OX-P were prepared as described previously (8, 12, 13). Dihydro-ZIP was prepared by treatment of ZIP with benzyl mercaptan in isopropanol for 24 hr.[2] *S*-Methyl-dihydro-ZIP and *S*-methyl-dihydro-ZIP-SO were prepared by methylation of dihydro-ZIP with diazomethane or CH_3I/KOH and subsequent oxidation with oxone using standard procedures (8, 13).

Subjects and Dosing Procedure. The protocol for this study was approved by the local institutional review board before initiation. Four normal healthy male volunteers participated in the study. After being informed of the purpose, design, and potential risks of the study, the volunteers gave written consent. They were confined to the Clinical Research Facility under continuous medical observation for 12 hr before dosing and until 264 hr after dosing. ZIP was administered as a 20 mg suspension in water containing a total of 47.8 μCi of ^{14}C and 90.3 μCi of ^{3}H as a single oral dose in the morning after a standard meal. Subjects were fasted 8 hr before consuming a standard breakfast.

Sample Collection. Urine was collected from each subject for 11 days at 0–4, 4–12, 12–24, 24–48, 48–72, 72–96, 96–120, 120–144, 144–168, 168–192, 192–216, 216–240, and 240–264 hr postdose. Feces were collected from time of dosing until 264 hr after dosing. The weight of urine and fecal samples was recorded. Blood was collected in tubes containing no preservatives, anticoagulant, or serum separator at the following times: 0 (just before dosing), 1, 2, 3, 4, 6, 8, 12, 16, 24, 36, 48, 72, 96, and 120 hr after drug administration. Blood was centrifuged within 1 hr after collection, and the serum was transferred to clean tubes.

Analysis of Radioactivity. Quantification of total radioactivity in urine and serum was determined by counting sample aliquots (200–500 μl, in triplicate) in a Wallac 1409 liquid scintillation counter using a "dual-label" $^{3}H/^{14}C$ program. Ecolite (+)-scintillation cocktail (5 ml) was used for determination of radioactivity in the samples. Factory-installed quench curves were used for determination of counting efficiencies for ^{3}H and ^{14}C.

Fecal samples were placed in Stomacher 400 bags and homogenized in water to a thick slurry using a Stomacher 400 Lab Blender (Cooke Laboratory Products, Alexandria, VA). Small aliquots (200–400 mg) were combusted using a United Technologies Packard Oxidizer model 306. Liberated $^{14}CO_2$ and $^{3}H_2O$ were trapped, and the radioactivity in the trapped samples was determined by liquid scintillation analysis. Packard Monophase S and Permafluor E+ scintillation cocktails were used for ^{3}H and ^{14}C, respectively. Combustion efficiencies were determined by combusion of ^{14}C and ^{3}H standards in an identical manner.

Quantification of ZIP in Serum. Serum concentrations of unchanged ZIP were determined by an LC/MS/MS assay (14). The limit of quantification was from 0.5 to 50 ng/ml, and the interassay precision was 9% or better. Pharmacokinetic parameters were determined using a pharmacokinetic computer program written in the RS/1 command language (RS/1 release 5.0.1; Bolt Beranek and Newman Software Products Corp., Cambridge, MA). The terminal phase rate constant (K_{el}) was determined from the beginning of the terminal phase to the last sampling time postdose by least squares regression analysis of the serum concentration-time data during terminal log-linear phase. Mean terminal phase half-life ($t_{1/2}$) was calculated as 0.693/mean K_{el}. The $AUC_{(0-t)}$ was calculated up to the last detectable concentration time point t using a trapezoidal approximation of area, and 0 as the time 0 concentration. C_{max} was the first occurrence of the peak serum concentration, and t_{max} was the earliest time at which C_{max} was observed.

Extraction of Metabolites from Biological Samples. A major portion of the radioactivity was recovered in the first 24 hr. Therefore, urine samples at 0–4, 4–12, and 12–24 hr postdose were pooled on the basis of volume collected, and pooled urine was used for the extraction and identification of metabolites. Pooled urine (10 ml, 0–24 hr) from each subject was diluted with acetate buffer (pH 5.0) and was applied to a preconditioned C_{18} Sep-Pak (Waters Associates, Milford, MA). The column was washed with water, and the metabolites were eluted with methanol. A small aliquot of the methanol solution was counted. The recovery of radioactivity was >95% from columns. The organic solvent was evaporated to dryness, and the residue was dissolved in 200 μl of methanol:ammonium acetate (1:4), and an aliquot (80 μl) was injected on HPLC. Serum (5 ml, 0–8 hr) was diluted with 10 ml of acetonitrile, and the precipitated protein was removed by centrifugation. The pellet was washed with an additional 2 ml of acetonitrile, and both supernatants were combined. The supernatant was concentrated, dissolved in 200 μl of mobile phase, and an aliquot (80 μl) was injected into the HPLC.

Enzyme Hydrolysis. Pooled urine sample (5 ml) was adjusted to pH 5 with sodium acetate buffer (0.1 M) and treated with 2500 units of β-glucuronidase/sulfatase. The mixture was incubated in a shaking water bath at 37°C for 12 hr and was extracted as described. Incubation of the urine sample without the enzyme served as a control.

HPLC. HPLC was conducted on a system that consisted of a Rheodyne injector (Cotati, CA) for manual injections, a LDC/Milton Roy constaMetric CM4100 gradient pump (Riviera Beach, FL), a Waters Lambda-Max model 481 UV detector (Milford, MA), a radioactivity monitor (β-RAM; Tampa, FL), and a SP 4200 computing integrator (Riviera Beach, FL). Chromatography was performed on a YMC basic HPLC column (4.6 mm × 250 mm, 5 μm) with a binary mixture of 20 mM ammonium acetate (pH 5.0, solvent A) and methanol (solvent B). The mobile phase initially consisted of solvent A/solvent B (90:10) for 10 min. It was then linearly programmed to solvent A/solvent B (20:80) over a period of 50 min, held under isocratic conditions for 7 min, and then programmed back to the starting solvent mixture over a period of 8 min. The system was allowed to equilibrate for ~10 min before making the next injection.

Quantitative Assessment of Metabolite Excretion. The quantification of fecal and urinary metabolites was conducted by measuring the radioactivity in the individual peaks that were separated on HPLC using β-RAM. The β-RAM provided an integrated printout in dpm and the percentage of the radiolabeled material, as well as peak representation. The β-RAM was operated in the homogeneous liquid scintillation counting mode with the addition of 4 ml/min of Ecolite (+)-scintillation cocktail to the eluent post-UV detection. For simultaneous monitoring of ^{3}H- and ^{14}C-labeled compounds, efficiencies of 37% for ^{3}H and 55% for ^{14}C were used, with a compensation for ^{14}C spillover into the ^{3}H window of 31%. These parameters were determined through separate injections of single-labeled standards. The radiochromatograms of metabolites in serum were generated by collecting fractions at 20-sec intervals and counting the fractions in a Wallac 1409 liquid scintillation counter using a "dual-labeled" $^{3}H/^{14}C$ program. The retention time of the radioactive peaks was compared with the synthetic standards, and characterization of the major metabolites was conducted by LC/MS/MS.

[2] S. Walinsky *et al.*, unpublished work.

TABLE I

Radiolabeled mass balance of ZIP in four male subjects after a single 20 mg dose of ^{14}C- and ^{3}H-ZIP

Percentage of ^{3}H and ^{14}C excreted in urine and feces from 0 to 264 hr

Time (hr postdose)	Urine		Feces		Total	
	^{3}H	^{14}C	^{3}H	^{14}C	^{3}H	^{14}C
0–4	0.89 ± 0.45	0.97 ± 0.49	—	—	0.90 ± 0.45	0.97 ± 0.49
4–12	8.31 ± 1.69	9.09 ± 1.81	—	—	8.32 ± 1.69	9.09 ± 1.80
12–24	4.00 ± 0.82	3.81 ± 0.87	15.14 ± 5.24	14.08 ± 4.62	19.15 ± 5.34	17.90 ± 4.60
24–48	2.67 ± 0.59	2.11 ± 0.55	28.65 ± 3.77	27.29 ± 4.00	31.32 ± 3.61	29.40 ± 3.78
48–72	1.16 ± 0.40	0.96 ± 0.30	8.47 ± 1.47	8.09 ± 1.28	9.63 ± 1.60	9.04 ± 1.35
72–96	0.72 ± 0.19	0.64 ± 0.16	4.97 ± 2.93	4.74 ± 2.82	5.70 ± 2.88	5.39 ± 2.80
96–120	0.60 ± 0.07	0.55 ± 0.07	2.75 ± 0.07	2.66 ± 0.08	3.35 ± 0.08	3.21 ± 0.08
120–144	0.51 ± 0.14	0.45 ± 0.11	2.25 ± 0.73	2.11 ± 0.69	2.75 ± 0.64	2.55 ± 0.62
144–168	0.57 ± 0.17	0.50 ± 0.13	1.67 ± 0.45	1.63 ± 0.42	2.24 ± 0.61	2.13 ± 0.55
168–264	1.15 ± 0.17	0.99 ± 0.17	4.20 ± 0.45	3.93 ± 0.80	5.35 ± 0.93	4.92 ± 0.85
Total	20.59 ± 0.96	20.07 ± 1.12	68.11 ± 4.77	64.52 ± 4.96	88.69 ± 4.72	84.59 ± 5.05

MS. Analysis of the metabolites was performed on a Perkin-Elmer-SCIEX API III HPLC/MS/MS system (Toronto, Ontario, Canada) using ion spray. The effluent from the HPLC column was split and ~50 μl/min was introduced into the ion spray interface. The remaining effluent was directed into the flow cell of the β-RAM. The β-RAM response was recorded in real time by the mass spectrometer that provided simultaneous detection of radioactivity and MS data. The delay in response between the two detectors was ~0.2 min, with the mass spectrometric response recorded earlier. The ion spray interface was operated at 6000 V, and the mass spectrometer was operated in the positive-ion mode. CID studies were performed using argon gas at a collision energy of 25 eV and a collision gas thickness of 3.5×10^{14} molecules/cm^2.

Results

Excretion. The percentage of radioactivity excreted in urine and feces of four human volunteers after oral administration of ^{3}H- and ^{14}C-ZIP is shown in table 1. Overall, 87 ± 4% of the radioactive dose (average of ^{3}H and ^{14}C) was recovered in urine and feces. The percentage of the radioactive dose excreted in urine and feces was 20.3 ± 1 and 66.3 ± 5%, respectively. Of all the radioactivity recovered in urine and feces, ~89% and 64% were excreted in the first 48 hr, respectively.

Pharmacokinetics. The mean serum concentration-time curves for total radioactivity and unchanged ZIP in human subjects after administration of a 20 mg dose of ^{3}H- and ^{14}C-ZIP are shown in fig. 2. Absorption of ZIP was rapid, as indicated by the early appearance of radioactivity in serum after oral administration. However, total radioactivity as a ^{14}C label was somewhat lower than the ^{3}H label in all subjects. The C_{max} of total radioactivity was reached at 6 hr postdose, except in one subject where C_{max} was reached at 4 hr postdose, and was 91.5 ± 25 ng-eq/ml (range: 61 ng-eq/ml to 119 ng-eq/ml) (table 2). Detectable concentration of radioactivity could be seen up to 16 hr in all four subjects.

The t_{max} value for unchanged ZIP was reached between 2 and 6 hr postdose, with a mean C_{max} of 45.4 ± 31 ng/ml (range: 28.8 to 62.0 ng/ml), half of that to total radioactivity (table 2). Similarly, the $AUC_{(0-16)}$ values for total radioactivity (mean: 724.6 ng-eq · hr/ml) were nearly 2-fold higher than those for the unchanged ZIP (mean: 335.7 ng · hr/ml). These data suggested that approximately one-half of the circulating radioactivity (average of ^{3}H and ^{14}C) was attributable to metabolites.

Metabolism. *Urine.* The representative profiles of metabolites in urine samples (0–24 hr) from human subjects after oral administration of ^{3}H- and ^{14}C-ZIP with on-line radioactivity monitoring of ^{14}C (*top panel*) and ^{3}H (*bottom panel*) are given in fig. 3. A total of 10

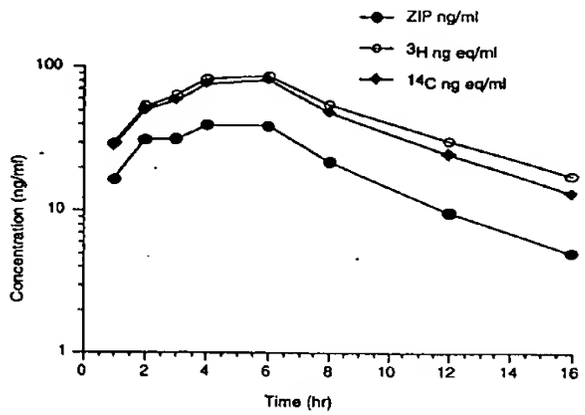

FIG. 2. *Mean serum concentration-time curves of total radioactivity and ZIP in male subjects.*

radioactive peaks were detected in the chromatograms. The radio-HPLC data are presented with the peak height normalized to that of the highest peak. Based on the radiolabel, the metabolites were classified into three categories: *1*) metabolites with only ^{3}H, *2*) metabolites containing only the ^{14}C label, and *3*) metabolites that contained both the labels. Metabolites with only one label, ^{3}H or ^{14}C, were identified as cleaved products and derived from benzisothiazole or oxindole moieties, respectively, and the metabolites that contained both the labels were from the intact molecule. Metabolites were quantified with on-line integration of the radiochromatographic peaks. The percentages of the metabolites excreted in relation to the total radioactivity in urine are presented in table 3. The identified metabolites accounted for >90% of the total radioactivity present in urine.

LC/MS (full scan) and tandem MS, such as precursor ion, product ion, CNL and MRM scanning techniques were used for the identification of metabolites (8,15–17). Product ion mass spectrum of ZIP (*m/z* 413) showed an intense ion at *m/z* 194. The ion at *m/z* 194 corresponds to a charge-initiated fragmentation of the aliphatic methylene carbon-piperazine nitrogen bond [$(OX—CH_2CH_2)^+$], with expulsion of the piperazine nitrogen-containing moiety as a neutral (219 Da). The assignment of this ion was verified by parallel CID spectrum of *m/z* 415 [$(M+H)^+$, ^{37}Cl] that gave the fragment ion at *m/z* 196. Thus, the scans for the precursors of *m/z* 194 and the neutral loss of 219 (MH-194) detected all of the metabolites that were modified on the

TABLE 2

Pharmacokinetic parameters of ZIP and total radioactivity in four male subjects after a single 20 mg dose of ^{3}H- and ^{14}C-ZIP

Subject ID	Unchanged Drug & Radioactivity	PK Parameters[a]				
		$AUC_{(0-t)}$	C_{max}	t_{max}	K_{el}	$t_{1/2}$
		ng-hr/ml	*ng/ml*	*hr*	*1/hr*	*hr*
610-0001	ZIP	344.5	44.0	2	0.217	3.20
	^{3}H radioactivity	723.3	88.0	6	0.169	4.10
	^{14}C radioactivity	677.7	87.2	6	0.192	3.61
	ZIP (%)	49.2	50.2			
610-0002	ZIP	289.9	28.8	2	0.161	4.31
	^{3}H radioactivity	672.6	66.4	6	0.131	5.31
	^{14}C radioactivity	594.4	60.9	6	0.149	4.65
	ZIP (%)	45.8	45.3			
610-0003	ZIP	325.0	62.0	4	0.194	3.57
	^{3}H radioactivity	729.5	115.2	4	0.152	4.56
	^{14}C radioactivity	647.0	104.0	4	0.178	3.90
	ZIP (%)	47.2	56.6			
610-0004	ZIP	391.5	54.0	6	0.215	3.23
	^{3}H radioactivity	956.1	118.7	6	0.162	4.27
	^{14}C radioactivity	849.6	110.4	6	0.181	3.82
	ZIP (%)	43.4	47.1			
Mean[b] ± CV (%)	ZIP	335.7 ± 12.5	45.4 ± 31.5	3.5 ± 54.7	0.197 ± 13.2	3.53
	^{3}H radioactivity	763.2 ± 16.4	94.5 ± 26	5.5 ± 18.2	0.153 ± 10.9	4.52
	^{14}C radioactivity	685.9 ± 15.9	88.4 ± 25	5.5 ± 18.2	0.175 ± 10.5	3.96
	ZIP (%)	46.3 ± 5.3	49.6 ± 10			

PK, pharmacokinetic; CV, coefficient of variation.

[a] C_{max} and $AUC_{(0-t)}$ values for radioactivity are expressed as ng-eq/ml and ng-eq · hr/ml, respectively, t = 16 hr.

[b] Geometric mean for $AUC_{(0-t)}$ and C_{max} and average for t_{max} and K_{el} and mean $t_{1/2}$ = 0.693/mean K_{el}.

TABLE 3

Percentage of metabolites of ZIP in human urine and serum

Metabolite No.	% of Radioactivity[a]	
	Urine	Serum
M1[b]	11.62	21.53[c]
M2[b]	4.56	
M3[b]	1.88	4.05
M3A[d]	15.35	3.40
M4[d]	24.72	2.03
M4A[d]	2.01	1.60
M5[b]	3.44	0.76
M6	9.11	3.99[e]
M7	5.20	
M8	2.56	1.15
M9	31.84	16.02[f]
M10	0.49	
M13	5.01	25.95

[a] Average of ^{14}C and ^{3}H labels.

[b] Only ^{3}H label.

[c] Mixture of **M1** and **M2**.

[d] Only ^{14}C label.

[e] Mixture of **M6** and **M7**.

[f] Mixture of **M9** and **M10**.

benzisothizol-piperazine moiety and oxindole ring, respectively. A parent ion scan of *m/z* 194 from a urine sample and the response from the radioactivity detector revealed the protonated molecular ions $(M+H)^+$ for seven metabolites (**M4A, M6, M7, M8, M9, M10,** and **M13**) (fig. 4). The molecular ions of remaining metabolites were determined by full-scan LC/MS. The structures of all the metabolites were determined from the interpretation of their product ion spectra and were confirmed by comparison of their HPLC retention times with those of synthetic standards.

Metabolites M1, M2, and **M3**. **M1, M2,** and **M3** had the retention times of 9:02, 9:30, and 14:43 (min:sec), respectively, on HPLC and were detected only in the ^{3}H chromatograms indicating that these metabolites were cleaved products and contained benzisothiazole moiety. Full-scan LC/MS of **M1** showed a strong signal for the protonated molecular ion at *m/z* 252, 32 Da higher than BITP, indicative of the addition of two oxygen atoms. The CID product ion spectrum of **M1** (*m/z* 252) showed the fragment ions at *m/z* 209 and 166, suggesting the presence of oxygen atoms on the benzisothiazole ring. **M1** coeluted with the authentic BITP-SO_2 on HPLC and had an identical CID spectrum. Based on these data, **M1** was identified as BITP-SO_2.

Full-scan LC/MS of **M2** showed the strong signal at *m/z* 236, 16 Da higher than BITP, suggesting the addition of an oxygen atom to the BITP. The CID product ion spectrum of **M2** (*m/z* 236) showed the fragment ions at *m/z* 220, 177, and 134. **M2** coeluted with the authentic BITP-SO on HPLC and had an identical CID spectrum. Based on these data, **M2** was identified at BITP-SO. **M3** exhibited an intense ion at *m/z* 266, 14 Da higher than **M1**. **M3** coeluted with synthetic BITP-SO_2 lactam and metabolite **M3** from rat urine (8). Thus, **M3** was identified as BITP-SO_2 lactam.

Metabolites M3A, M4, and M4A. **M3A, M4,** and **M4A** had the retention times of 17:17, 21:54, and 26:45 (min:sec), respectively, on HPLC and had only ^{14}C label indicating that these metabolites were cleaved products and contained an oxindole moiety. A full-scan LC/MS of **M3A** showed the ammoniated $(M+NH_4)$ adduct ions at

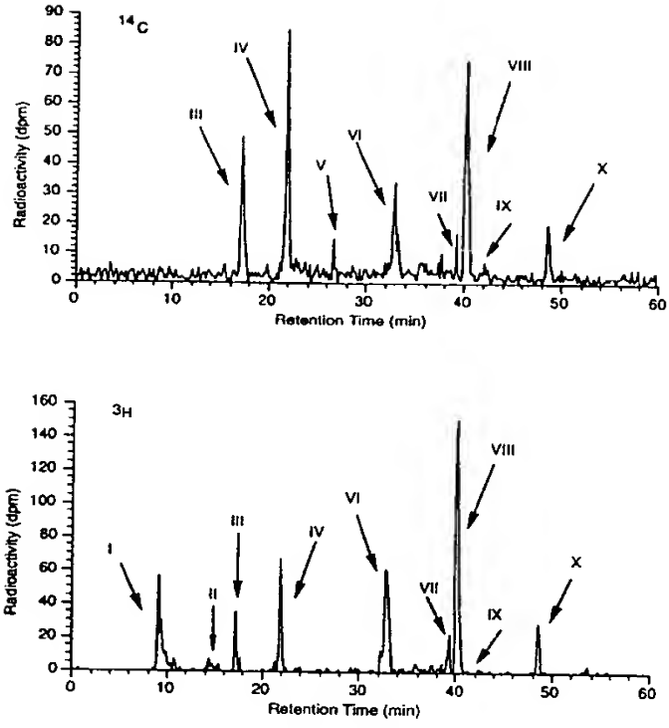

FIG. 3. *HPLC radiochromatograms of ZIP metabolites in human urine.*

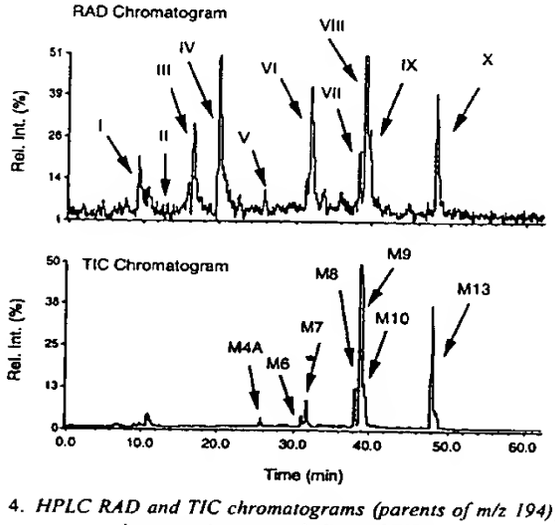

FIG. 4. *HPLC RAD and TIC chromatograms (parents of m/z 194) for human urinary metabolites of ZIP.*

Rel. Int., relative intensity.

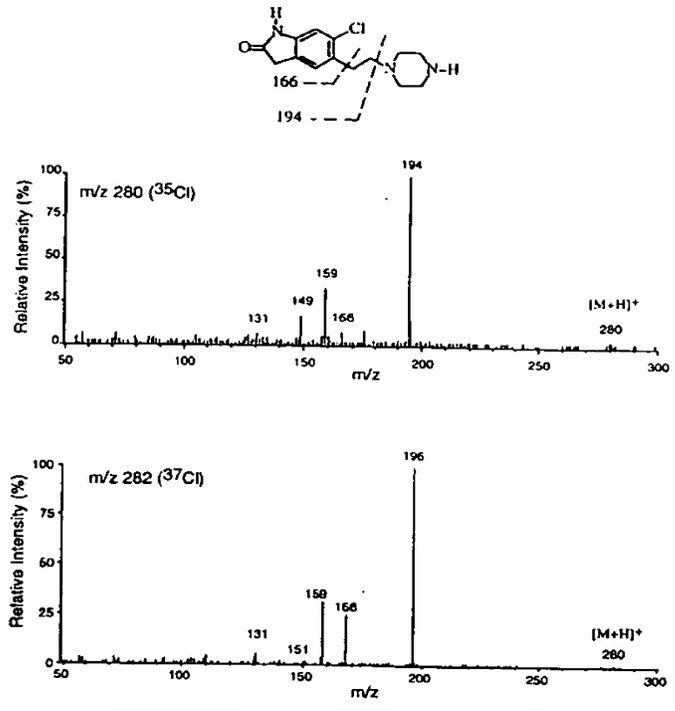

FIG. 5. *CID product ion spectra of human urinary metabolite* M4A.

m/z 419 (421, ^{37}Cl). Treatment of the urine sample with β-glucuronidase resulted in the disappearance of M3A and in the increase of peak area corresponding to M4 (not shown). These results suggested that M3A was a glucuronide conjugate of M4. The CID product ion spectrum of *m/z* 419 showed the structurally significant fragment ions at *m/z* 226, 209, 180, and 131. Based on these data, M3A was identified as a glucuronide conjugate of M4.

A full-scan LC/MS of M4 showed an ammoniated adduct ion $(M+NH_4)^+$ at *m/z* 243 (245, ^{37}Cl) and a protonated molecular ion at *m/z* 226 (228, ^{37}Cl). The CID product ion spectrum of M4 (*m/z* 243) showed a characteristic fragment ion at *m/z* 180, loss of 46 Da from the protonated molecular ion, suggesting that a free carboxylic acid group was present in the molecule. M4 coeluted with synthetic OX-AA on HPLC and had an identical CID spectrum. Based on these data, M4 was identified as OX-AA.

The parent scan of *m/z* 194 corresponding to M4A showed the protonated molecular ion at *m/z* 280, 134 mass units lower than the drug, thus suggesting that the benzisothiazole moiety was removed from the parent drug. The CID product ion spectrum of M4A showed the prominent fragment ions at *m/z* 194, 166, and 159 (fig. 5). The ions at *m/z* 194 and 159 suggested that the oxindole moiety was unchanged. These fragmentations were verified by parallel CID spectrum of *m/z* 282 $[(M+H)^+, {}^{37}Cl]$, which gave the fragment ions at *m/z* 196, 168, and 159. M4A coeluted with synthetic standard and had an identical CID spectrum. Based on these data, M4A was identified as OX-P.

Metabolites M5, M6, and M7. Peak VI had a retention time of 32:53 min and was found to be a mixture of three metabolites (M5, M6, and M7). One of the metabolites M5 showed a protonated molecular ion at *m/z* 220, and its CID product ion spectrum showed a fragment ion at *m/z* 177, with a loss of 43 Da; the same was true of BITP. M5 coeluted with synthetic BITP standard and had an identical CID spectrum. Based on these data, M5 was identified as BITP.

The second metabolite in peak VI showed a protonated molecular ion at *m/z* 445 (447, ^{37}Cl), 32 Da higher than the parent drug, suggesting the addition of two oxygen atoms to the molecule. Its CID spectrum (*m/z* 445) showed two very useful prominent fragment ions at *m/z* 280 and 166. The ion at *m/z* 280 corresponds to a charge-initiated fragmentation of the piprazinyl nitrogen-benzisothiazole carbon bond, with the expulsion of the benzisothiazole moiety as a neutral molecule. The ion at *m/z* 166 was resulted by the cleavage of the same nitrogen-carbon bond, but with charge retention on the benzisothiazole moiety as outlined in fig. 6. The assignment of these ions was confirmed by parallel CID spectrum of *m/z* 447 $[(M+H)^+, {}^{37}Cl]$, which gave the fragment ions at *m/z* 282 and 166. These results

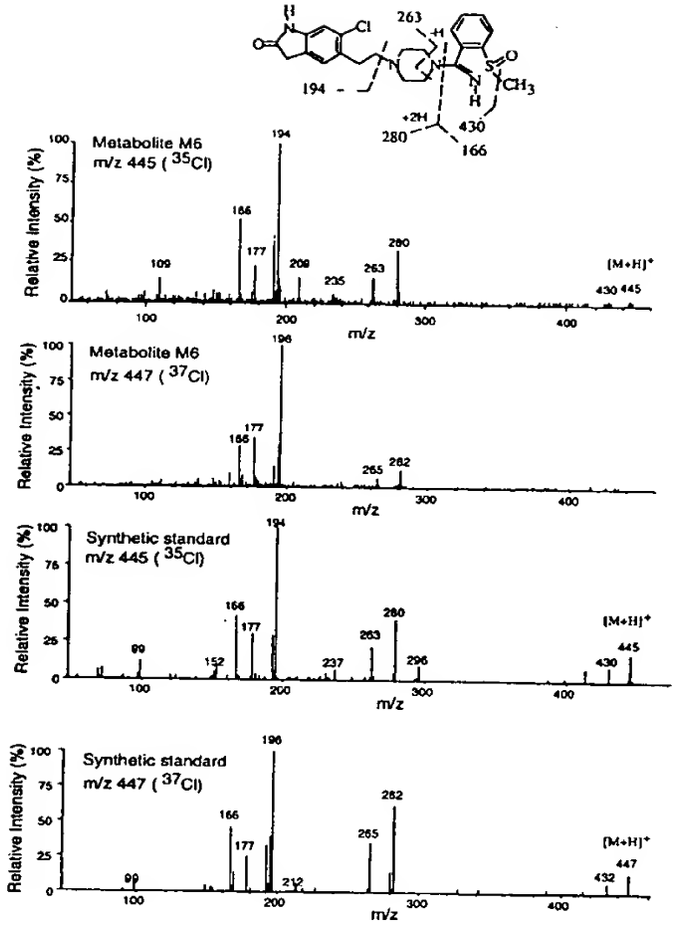

FIG. 6. *CID product ion spectra of human urinary metabolite* M6 and synthetic standard.

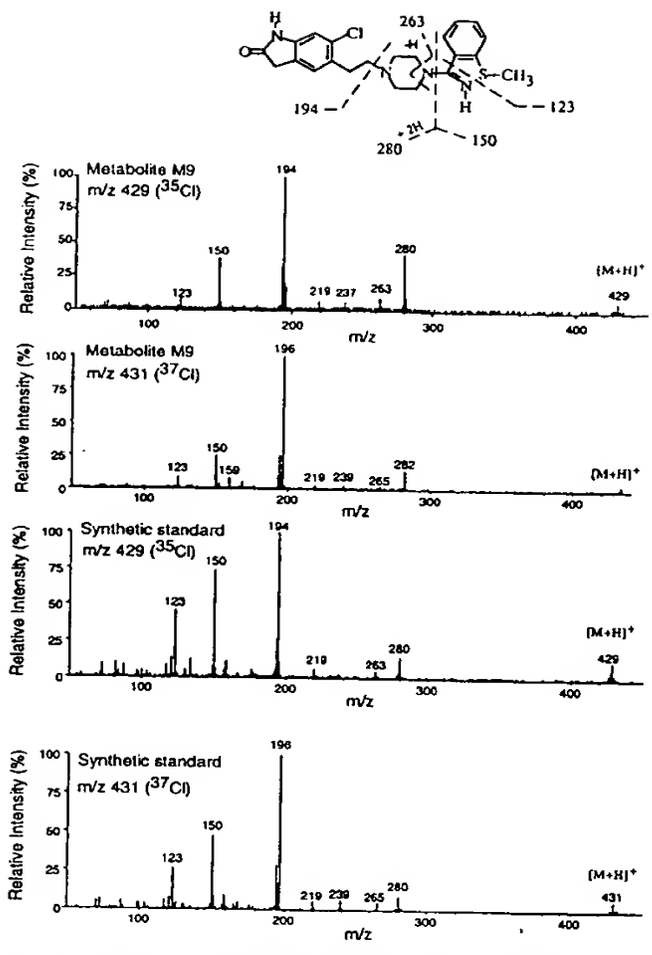

FIG. 7. *CID product ion spectra of human urinary metabolite* M9 and synthetic standard.

suggested that the addition of oxygen atoms had occurred on the benzisothiazole moiety. The presence of other characteristic fragment ions at *m/z* 194 and 263 in its CID spectrum further suggested that oxidation had occurred remote from the oxindole part of the molecule. A very characteristic fragment ion at *m/z* 430, loss of 15 Da from the parent molecule, indicated the presence of a methyl group. **M6** did not coelute with the synthetic ZIP-SO_2 standard on HPLC. Treatment of the urine sample with aqueous $TiCl_3$ resulted in the disappearance of **M6** and the increase in peak area of **M9**, suggesting that **M6** was either *N*-oxide or *S*-oxide of **M9**. The reaction of the urine sample with MTBSTFA or diazomethane did not change the retention time of metabolite **M6**, suggesting that a free hydroxyl group was not present. **M6** coeluted with synthetic *S*-methyl-dihydro-ZIP-SO and had an identical CID product ion spectrum. Based on these data, **M6** was identified as *S*-methyl-dihydro-ZIP-SO.

The third metabolite in peak **VI** indicated a protonated molecular ion at *m/z* 447, 34 Da higher than the parent drug, suggesting that the molecule had undergone monooxidation and an addition of water. Its CID spectrum showed the fragment ions at *m/z* 280, 263, 194, and 168. The prominent fragment ion at *m/z* 168, 34 Da higher than the BITP, suggested the oxidation at the benzisothiazole moiety. It was further supported by the presence of other fragment ions at *m/z* 280, 263, and 194. Its retention time on HPLC was similar to that of metabolite **M7** obtained from rat urine (8). Based on these data, **M7** was characterized as dihydro-ZIP-O_2.

Metabolite M8. **M8** indicated a protonated molecular ion at *m/z* 445, 32 Da higher than the parent drug, suggesting that the molecule had undergone two oxidations. Its CID spectrum showed an abundant fragment ion at *m/z* 194, indicating that the oxidation had occurred remote from the oxindole part of the molecule. It coeluted with authentic ZIP-SO_2 on HPLC and had an identical CID spectrum. Based on these data, **M8** was identified as ZIP-SO_2.

Metabolite M9. **M9** had a retention time of 40:09 min and showed a protonated molecular ion at *m/z* 429, 16 Da higher than the parent drug, suggesting that it was a monooxidation product of ZIP. Its CID product ion spectrum showed two very useful prominent fragment ions at *m/z* 280 and 150, suggesting the presence of oxygen on the benzisothiazole moiety (fig. 7). The assignment of these ions was confirmed by parallel CID spectrum of *m/z* 431 (MH^+, ^{37}Cl), which gave the fragment ions at *m/z* 282 and 150. The other characteristic fragment ions at *m/z* 194 and 159 also suggested that the addition of oxygen had occurred remote from the oxindole part of the molecule. The retention time of **M9** was different from those of the synthetic ZIP-SO and 5-OH-ZIP standards. Treatment of urine sample with aqueous $TiCl_3$ or MTBSTFA did not change the retention time or the CID spectrum of metabolite **M9**. This eliminated the possibility of *N*-oxide or hydroxy-ZIP. **M9** coeluted with synthetic *S*-methyl-dihydro-ZIP and had identical CID product ion spectrum. Based on these data, **M9** was identified as *S*-methyl-dihydro-ZIP.

Metabolite M10. **M10** had a retention time of 41:02 min and

TABLE 4

MRM ions used to detect metabolites of ZIP in human serum

Metabolite No.	MRM Conversion
	m/z
M1	252→209
M2	236→150
M3	266→209
M4	226→180
M4A	280→194
M5	220→177
M6	445→194, 445→166
M7	447→194, 447→168
M8	445→194
M9	429→194, 429→150
M10	429→194, 429→99
M13	413→194

indicated a protonated molecular ion at *m/z* 429, 16 Da higher than the parent drug, suggesting that a single atom of oxygen had been added to the molecule. Its CID product ion spectrum showed fragment ions at *m/z* 194 and 232, indicating that the oxindole moiety was unchanged. The other fragment ion at *m/z* 99 $(HNC_4H_8N{=}CH_2)^+$ suggested that the piperazine ring was unsubstituted. **M10** coeluted with synthetic ZIP-SO on HPLC and had an identical CID product ion spectrum. Based on these data, **M10** was identified as ZIP-SO.

Metabolite M13 (Unchanged Drug). **M13** gave a protonated molecular ion at *m/z* 413. Its CID spectrum showed the prominent fragment ions at *m/z* 194, 177, and 166. It coeluted with authentic parent drug on HPLC and had an identical CID product ion specrum. Based on these data, **M13** was identified as unchanged drug.

Metabolites in Serum. The serum samples (0–8 hr) from each subject were pooled, diluted with acetonitrile, and centrifuged. A small aliquot of supernatant and pellet was counted. Approximately 83% of the total radioactivity was recovered in the supernatant. A total of 10 radioactive peaks were detected in the HPLC radiochromatogram of a serum sample (not shown). The metabolites were quantified by counting the radioactivity of individual peaks that were separated on HPLC. The percentages of circulating metabolites in relation to the total radioactivity observed in serum are presented in table 3.

Metabolites were identified by ion-spray LC/MS/MS using MRM technique and confirmed by compariosn of their retention times on HPLC with synthetic standards and/or with metabolites obtained from human urine. ZIP (**M13**) and a total of 12 metabolites (**M1, M2, M3, M3A, M4, M4A, M5, M6, M7, M8, M9,** and **M10**) were identified in serum and were similar to those found in human urine (tables 3 and 4).

Discussion

ZIP labeled with ^{14}C at C-2 position of the ethyl group attached to the piperazinyl nitrogen, and ^{3}H at the C-7 position of the benzisothiazole was administered orally to human subjects. After 10 days, the fecal and urinary routes accounted for essentially all of the administered dose. The total amount excreted in urine was 20%. The urinary recovery of the dose was similar to total recovery in bile and urine of dogs, suggesting that at least 20% of the drug was absorbed in humans (9). The serum concentrations of total radioactivity were greater than the parent compound at all time points. This suggested the early formation of metabolites. The serum concentration-time curves for unchanged ZIP in this study were very similar to those previously seen after oral administration to humans (6, 18).

ZIP was extensively metabolized, and only a small percentage of the unchanged drug was found in urine. A total of 10 radioactive peaks were detected in the radiochromatogram. The identification of metabolites in a complex biological matrix, such as urine, offers an analytical challenge to separate the different metabolites from each other, to separate compounds from the urine matrix, and to combine the separation with a sensitive detection method that gives structural information. We have used LC/MS/MS (19–22) in combination with on-line radioactivity monitoring (23). Both the radioactivity and MS data were acquired in the same time domain by a single data system that facilitated the matching of the two types of information. Using the responses from TIC and RAD, we have identified metabolites accounting for >90% of total radioactivity present in urine. The identities of major metabolites were confirmed by chromatographic comparisons with synthetic standards.

Based on the structures of metabolites, a plausible scheme for the biotransformation pathways of ZIP in humans is shown in fig. 8. The major routes of metabolism involved *N*-dealkylation of the ethyl side chain attached to the piperazinyl nitrogen (**M1, M2, M3, M3A, M4,** and **M5**), oxidation at sulfur resulting in the formation of sulfoxide and sulfone (**M8** and **M10**), reductive cleavage of the benzisothiazole moiety followed by methylation (**M6** and **M9**), and hydration of the C=N bond and oxidation at the sulfur or dearylation of the benzisothiazole moiety (**M4A** and **M7**). The first route, *N*-dealkylation, was analogous to that observed for the structurally related drugs (10, 24–26). The formation of sulfoxide and sulfone is common with sulfur-containing drugs (10, 27). The affinities of the sulfoxide and sulfone metabolites for 5-HT_2 and D_2 receptors are low with respect to ZIP, and are thus unlikely to contribute to its antipsychotic effects.[3]

The major *N*-dealkylation products of ZIP were OX-AA (**M4**), BITP (**M5**), BITP-SO (**M2**), BITP-SO_2 (**M1**), and the corresponding lactam (**M3**). These metabolites accounted for 44% of total radioactivity present in urine. Unlike rats, metabolite OX-AA (**M4**) derived from this route was found to be capable of undergoing subsequent phase II metabolism by conjugation with glucuronic acid (**M3A**). The formation of BITP-SO and BITP-SO_2 suggests that the benzisothiazole moiety is more susceptible to oxidation at sulfur than it is to aromatic hydroxylation.

The important findings in the present study were the formation of several novel metabolites, **M4A** (*N*-debenzisothiazolylation), **M6, M7,** and **M9**. The metabolites **M4A** and **M7** were formed by the addition of water and subsequent *N*-dearylation or the cleavage of the C—N bonds of the benzisothiazole moiety and were identified as OX-P and dihydro-ZIP-O_2, respectively. A possible mechanism for the formation of **M4A** and **M7** can be postulated as follows. Hydration of the C—N double bond of ZIP would result in a carbinoldiamine intermediate that could be hydrolytically rearranged by a reaction identical to the second step of *N*-dealkylation (28–30). Either of the two C—N bonds could be cleaved to yield OX-P or hydrated-ZIP. Unlike rats, both the metabolites were identified in human urine, suggesting that the cleavage was not selective (8). Hydrated-ZIP was found to be further oxidized at sulfur to form **M7**. The results of this study do not indicate whether hydration of the benzisothiazole occurs before or after the oxidation at the sulfur. But it seems reasonable to propose that the addition of water to the benzisothiazole moiety would be more likely to occur after oxidation of the sulfur atom to the sulfoxide, because this would render the heterocycle more electrophilic and thus more prone to hydration (fig. 9).

The other novel metabolic pathway of ZIP was the formation of metabolites **M6** and **M9**. MS data suggested that the metabolites **M6** and **M9** were resulted by the addition of 16 and 32 mass units, respectively, on the benzisothiazole moiety other than sulfur oxida-

[3] S. Zorn *et al.*, unpublished work.

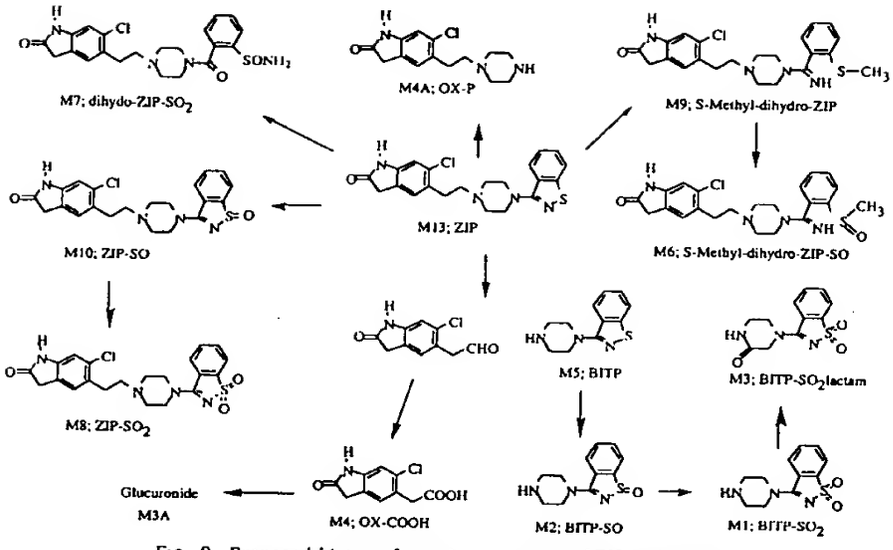

FIG. 8. *Proposed biotransformation pathways of ZIP in humans.*

tion. Based on these data, three structures were originally considered for **M9:** oxidation at the nitrogen of the benzisothiazole ring to form ZIP-*N*-oxide, aromatic hydroxylation of the benzisothiazole moiety (OH-ZIP), and reductive cleavage of the benzisothiazole, followed by methylation of the resulting thiophenol (*S*-methyl-dihydro-ZIP). Further sulfur oxidation of **M9** could give metabolite **M6.** Although, there are several investigational pharmaceutical compounds containing a benzisothiazole structure (13, 31, 32), but to our knowledge, *N*-oxidation, aromatic hydroxylation and/or reductive cleavage of the benzisothiazoles have not been reported. However, the oxidation of two heterocyclic atoms in an aromatic ring has been reported (33), whereas 4,5-dimethylthiazol-*N*-oxide-*S*-oxide was identified as a metabolite of chloromethiazole in humans. Therefore, the possibility of *N*-oxidation or aromatic hydroxylation of benzisothiazole ring was studied by reduction with $TiCl_3$ (34) and formation of silyl derivative (35), respectively. Both metabolites **M6** and **M9** were unaffected by the reaction of MTBSTFA, indicating that no free hydroxyl group was present. Treatment of urine sample with aqueous $TiCl_3$ resulted in the reduction of metabolite **M6** and the increase in peak area of **M9.** These data suggested that **M6** was a sulfur oxidation product of **M9,** and ruled out the possibility of **M9** being an *N*-oxide. Therefore, **M6** and **M9** were characterized as *S*-methyl-dihydro-ZIP-SO and *S*-methyl-dihydro-ZIP, respectively. Recently, *in vitro* studies of ZIP using human liver homogenate have demonstrated that the formation of these metabolites required the presence of *S*-adenosyl-methionine, an essential cofactor for the methylation of thiols, in the incubation medium (36). In an attempt to confirm further this route of metabolism, synthetic standards of *S*-methyl-dihydro-ZIP and *S*-methyl-dihydro-ZIP-SO were prepared by treatment of dihydro-ZIP with diazomethane or CH_3I/KOH and subsequent oxidation with oxone. Metabolites **M6** and **M9** coeluted with synthetic standards on HPLC and showed identical mass spectral characteristics (figs. 6 and 7).

Based on these results, we concluded that **M6** and **M9** were due to reductive cleavage of the benzisothiazole ring. Similar cleavage has been reported for the compounds possessing a 1,2-benzisoxazole ring structure, risperidone (37), zonisamide (38), iloperidone (39), and CP-118,954 (40). Reductive cleavage of benzisoxazoles resulted in the formation of an intermediate imine that is hydrolyzed nonenzymatically to a stable ketone. But, in ZIP, the intermediate amidine was not identified due to its instability under acidic conditions.

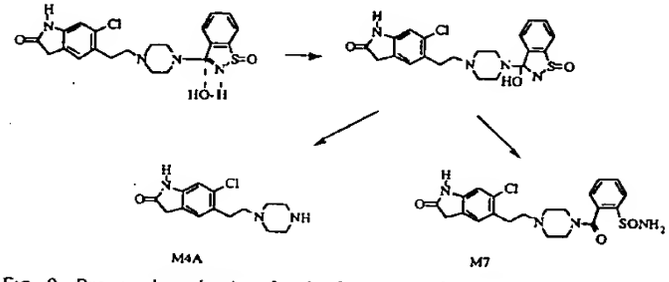

FIG. 9. *Proposed mechanism for the formation of metabolite* **M4A** and **M7.**

The formation of metabolites **M6** and **M9** involves two steps that may be catalyzed by two different enzymes. We do not presently know which enzymes are involved in reduction of the benzisothiazole. The opening of the benzisoxazole ring of risperidone was attributed to the reduction by gut microflora (37). The reductive ring opening is a reaction of dihydrogenation and as such must involve transfer of two electrons. It has recently been shown that the reductive ring opening in zonisamide is catalyzed mainly by a specific cytochrome P450 enzyme (CYP3A) in human and rat liver microsomes under anaerobic conditions (41, 42). Because ring-cleaved metabolites of ZIP were found in both urine and serum, we believe that the opening of the benzisothiazole ring is also mediated by liver enzymes. Further studies to determine the enzymes involved in the formation of these metabolites are currently under investigation.

In summary, the clearance of ZIP in human was by both phase I and phase II metabolism followed by elimination. The use of two labels and the presence of a chlorine atom were very helpful in identifying the metabolites and interpretation of their mass spectra. In addition to *N*-dealkylation and sulfur oxidation, two novel metabolic pathways were proposed for ZIP. The identification of these metabolic pathways of ZIP will have relevance to understanding the metabolism of other benzisothiazolepiperazine drugs. The identified metabolites described herein account for ~97% and 64% of the total radioactivity extracted from urine (0–24 hr) and serum (0–8 hr), respectively.

Acknowledgments. We would like to thank Dr. Keith McCarthy, Mr. Harry Howard, Dr. Stan Walinsky, and Mr. C. Sklavounos for

providing radiolabeled ZIP and synthetic standards; Dr. Benjamin Levy, National Medical Research Corporation (Hartford, CT), for conducting the dosing and sample collections; Mr. Wayne Anderson for technical assistance; and Drs. Hassan Fouda and Robert Ronfeld for helpful suggestions.

References

1. H. R. Howard, C. Prakash, and T. F. Seeger: Ziprasidone hydrochloride. *Drugs of the Future* **19**, 560–563 (1994).
2. H. R. Howard, J. A. Lowe III, T. F. Seeger, P. A. Seymour, S. H. Zorn, P. R. Maloney, F. E. Ewing, M. E. Newman, A. W. Schmidt, J. S. Furman, G. C. Robinson, E. Jackson, C. Johnson, and J. Morrone: 3-Benzisothiazolyl-piperazine derivatives as potential atypical antipsychotic agents. *J. Med. Chem.* **39**, 143–148 (1996).
3. T. F. Seeger, P. A. Seymour, A. W. Schmidt, S. H. Zorn, D. W. Schulz, L. A. Lebel, S. McLean, V. Guanowsky, H. R. Howard, J. A. Lowe III, and J. Heym: Ziprasidone (CP-88,059): a new antipsychotic with combined dopamine and serotonin receptor antagonist activity. *J. Pharmacol. Exp. Ther.* **275**, 101–113 (1995).
4. S. H. Zorn, T. F. Seeger, P. A. Seymour, A. W. Schmidt, D. W. Schulz, L. A. Lebel, S. McLean, V. Guanowsky, H. R. Howard, J. A. Lowe III, and J. Heym: Ziprasidone (CP-88,059) preclinical pharmacology review. *Jpn. J. Neuropsychopharmacol.* **17**, 701–707 (1995).
5. K. P. Gunn: Ziprasidone; safety and efficacy. *Schizophr. Res.* **18**, 132–133 (1996).
6. J. J. Miceli, T. Hunt, M. J. Cole, and K. D. Wilner: The pharmacokinetics of CP-88,059 in healthy male volunteers following oral and intravenous administration. *Clin. Pharmacol. Ther.* **55**, 142 (1994).
7. T. A. Smolarek and T. Morse: Pharmacokinetic and disposition studies of ziprasidone, a new antipsychotic. In "Proceedings of the European Conference on Specificity and Variability in Drug Metabolism," p. 27 (abstr.). Besanco, France 1995.
8. C. Prakash, A. Kamel, W. Anderson, and H. Howard: Metabolism and excretion of the antipsychotic drug ziprasidone in rat following oral administration of a mixture of ^{14}C- and ^{3}H-labeled ziprasidone. *Drug Metab. Dispos.* **25**, 206–218 (1997).
9. C. Prakash, A. Kamel, and W. Anderson: Biotransformation of antipsychotic drug ziprasidone in dogs. In "Proceedings of the 4th International Society for the Study of Xenobiotics," p. 312 (abstr.). Seattle, WA, 1995.
10. H. K. Jajoo, R. F. Mayol, L. J. Klunk, and I. A. Blair: Characterization of *in vitro* metabolites of the antipsychotic drug tiospirone by mass spectrometry. *Biomed. Environ. Mass Spectrom.* **19**, 281–285 (1990).
11. R. F. Mayol, H. K. Jajoo, L. J. Klunk, and I. A. Blair: Metabolism of the antipsychotic drug tiospirone in humans. *Drug Metab. Dispos.* **19**, 394–399 (1991).
12. H. R. Howard, K. D. Shenk, T. A. Smolarek, M. H. Marx, J. H. Windels, and R. W. Roth: Synthesis of ^{3}H- and ^{14}C-labeled CP-88,059: a potent atypical antipsychotic agent. *J. Labelled Compd. Radiopharm.* **34**, 117–125 (1994).
13. J. Cippolina, E. H. Ruediger, J. S. New, M. A. Wire, T. A. Shepherd, D. W. Smith, and J. P. Yevich: Synthesis and biological activity of the putative metabolites of the atypical antipsychotic agent tiospirone. *J. Med. Chem.* **34**, 3316–3328 (1991).
14. H. G. Fouda, K. Navetta, E. Luther, and R. P. Schneider: Quantitative determination of the antipsychotic agent CP-88, 059 in human serum by HPLC/MS/MS. In "Proceedings of the 41st American Society for Mass Spectrometry Conference on Mass Spectrometry and Allied Topics," p. 326 (abstr.). San Francisco, CA, 1993.
15. T. A. Baillie: Advances in the application of mass spectrometry to studies of drug metabolism, pharmacokinetics and toxicology. *Int. J. Mass Spectrom. Ion Proc.* **118/119**, 289–314 (1992).
16. C. Fenselau: Tandem mass spectrometry: the competitive edge for pharmacology. *Annu. Rev. Pharmacol. Toxicol.* **32**, 555–578 (1992).
17. J. V. Johnson, M. S. Lee, M. R. Lee, H. O. Brotherton, and R. A. Yost: Triple quadrupole MS/MS in biomedical research. In "Mass Spectrometry in Biomedical Research" (S. J. Gaskell, ed.), pp. 459–475. John Wiley & Sons Ltd., New York, 1986.
18. J. J. Miceli, R. A. Hanson, A. C. Johnson, and K. D. Wilner: Single and multiple dose pharmacokinetics of ziprasidone in healthy subjects. *Pharm. Res.* **12**, S-392 (1995).
19. K. M. Straub, P. Rodevicz, and C. Gravic: Metabolite mapping of drugs: rapid screening techniques for xenobiotics metabolites with MS/MS techniques. *Xenobiotica* **17**, 417–422 (1987).
20. W. M. Muck and J. D. Henion: High performance liquid chromatography/tandem mass spectrometry: its use for the identification of staozolol and its major metabolites in human and equine urine. *Biomed. Environ. Mass Spectrom.* **19**, 37–51 (1990).
21. J. J. Vrbanac, I. A. O'Leary, and L. Baczynski: Utility of the parent-neutral loss scan screening technique: partial characterization of urinary metabolites of U-78875 in monkey urine. *Biol. Mass Spectrom.* **21**, 517–522 (1992).
22. S. Naylor, M. Kajbaf, J. H. Lamb, M. Jahanshahi, and J. W. Gorrod: An evaluation of tandem mass spectrometry in drug metabolism studies. *Biol. Mass Spectrom.* **22**, 388–394 (1993).
23. H. G. Fouda, M. Avery, and K. Navetta: Simultaneous HPLC radioactivity and mass spectrometry monitoring: a drug metabolism application. In "Proceedings of the 41st American Society for Mass Spectrometry Conference on Mass Spectrometry and Allied Topics," p. 49 (abstr.). San Francisco, CA, 1993.
24. H. K. Jajoo, R. F. Mayol, J. A. Labudde, and I. A. Blair: Metabolism of the antianxiety drug buspirone in human subjects. *Drug Metab. Dispos.* **17**, 634–640 (1989).
25. H. K. Jajoo, R. F. Mayol, J. A. Labudde, and I. A. Blair: Metabolism of the antianxiety drug buspirone in the rat. *Drug Metab. Dispos.* **17**, 625–633 (1989).
26. K. B. Oseekey, S. G. Wood, L. F. Chasseaud, and M. Chung: Pharmacokinetics and metabolism of tandospirone in man. *Pharm. Res.* **9**, S-300 (1992).
27. B. Testa and P. Jenner: "Drug Metabolism: Chemical and Biochemical Aspects," pp. 76–77. Marcel Dekker, New York, 1976.
28. H. Uheleke: Metabolism of drugs as cause of efficacy, side effects and toxicity. *Prog. Drug Res.* **15**, 147–203 (1973).
29. H. Oelschlager, and M. Al Shaik: N-oxidation of alicyclic amines. In "Biological Oxidation of Nitrogens in Organic Molecules" (J. W. Gorrod and L. A. Damani, eds.), pp. 60–75. Ellis Horwood Ltd., Chichester, UK, 1985.
30. T. R. Fukuto: Metabolism of carbamate insecticides. *Drug Metab. Rev.* **1**, 117–151 (1972).
31. V. Franke, F. Frickel, J. Gries, H. D. Lehmann, D. Lenke, and U. Ohnsorge: New β-sympatholytic agents: synthesis and pharmacological activity of isomeric benzthiazole and benzoxazole derivatives. *Arzneim.-Forsch.* **30**, 1831–1838 (1980).
32. N. J. Hrib, J. G. Jurcak, F. P. Huger, C. L. Errico, and R. W. Dunn: Synthesis and biological evaluation of a series of substituted N-alkoxyimides and amides as potential atypical antipsychotic agents. *J. Med. Chem.* **34**, 1068–1072 (1991).
33. C. P. Offen, M. J. Frearson, and K. Wilson: 4,5-Dimethylthiazole-N-oxide-S-oxide: a metabolite of chlormethiazole in man. *Xenobiotica* **15**, 503–511 (1985).
34. J. M. McCall and R. E. Tenbrink: Heterocyclic N-oxide reduction by titanium chloride. *Synthesis* 335–336 (1975).
35. C. Prakash, S. Saleh, and I. A. Blair: Selective removal of phenolic and alcoholic silyl ethers. *Tetrahedron Lett.* **35**, 7565–7568 (1994) and references therein.
36. C. Prakash, A. Kamel, and D. Cui: Identification of novel benzisothiazole ring cleaved metabolites of ziprasidone. *Drug Metab. Dispos.* **25**, 897–901 (1997).
37. G. Mannens, M. L. Huang, W. Meuldermans, J. Hendrickx, R. Woestenborghs, and J. Heykants: Absorption, metabolism and excretion of risperidone in humans. *Drug Metab. Dispos.* **21**, 1134–1140 (1993).

38. D. D. Stiff and M. A. Zemaitis: Metabolism of the anticonvulsant agent zonisamide in the rat. *Drug Metab. Dispos.* **18**, 888–894 (1990).
39. A. E. Mutlib, J. T. Strupczewski, and S. M. Chesson: Application of hyphenated LC/NMR and LC/MS techniques in rapid identification of *in vitro* and *in vivo* metabolites of iloperidone. *Drug Metab. Dispos.* **23**, 951–964 (1995).
40. C. Prakash and D. Cui: Characterization of metabolites of CP-118,954 in rat urine and bile by liquid chromatography/tandem mass spectrometry with simultaneous radioactivity monitoring. In "Proceedings of the 44th American Society for Mass Spectrometry Conference on Mass Spectrometry and Allied Topics," p. 251 (abstr.). Portland, OR, 1996.
41. H. Nakasa, M. Komiya, S. Ohmori, T. Rikihisa, M. Kiuchi, and M. Kitada: Characterization of human liver microsomal cytochrome P-450 involved in the reductive metabolism of zonisamide. *Mol. Pharmacol.* **44**, 216–221 (1993).
42. H. Nakasa, M. Komiya, S. Ohmori, T. Rikihisa, and M. Kitada: Rat liver microsomal cytochrome P-450 responsible for the reductive metabolism of zonisamide. *Drug Metab. Dispos.* **21**, 777–801 (1993).